LBL-27478

Lawrence Berkeley Laboratory
UNIVERSITY OF CALIFORNIA

Accelerator & Fusion Research Division

Presented at the Third Advanced ICFA Beam Dynamics Workshop on Beam-Beam Effects in Circular Colliders, Novosibirsk, USSR, May 29–June 3, 1989

Renormalization Theory of Beam-Beam Interaction in Electron-Positron Colliders

Y.H. Chin

July 1989

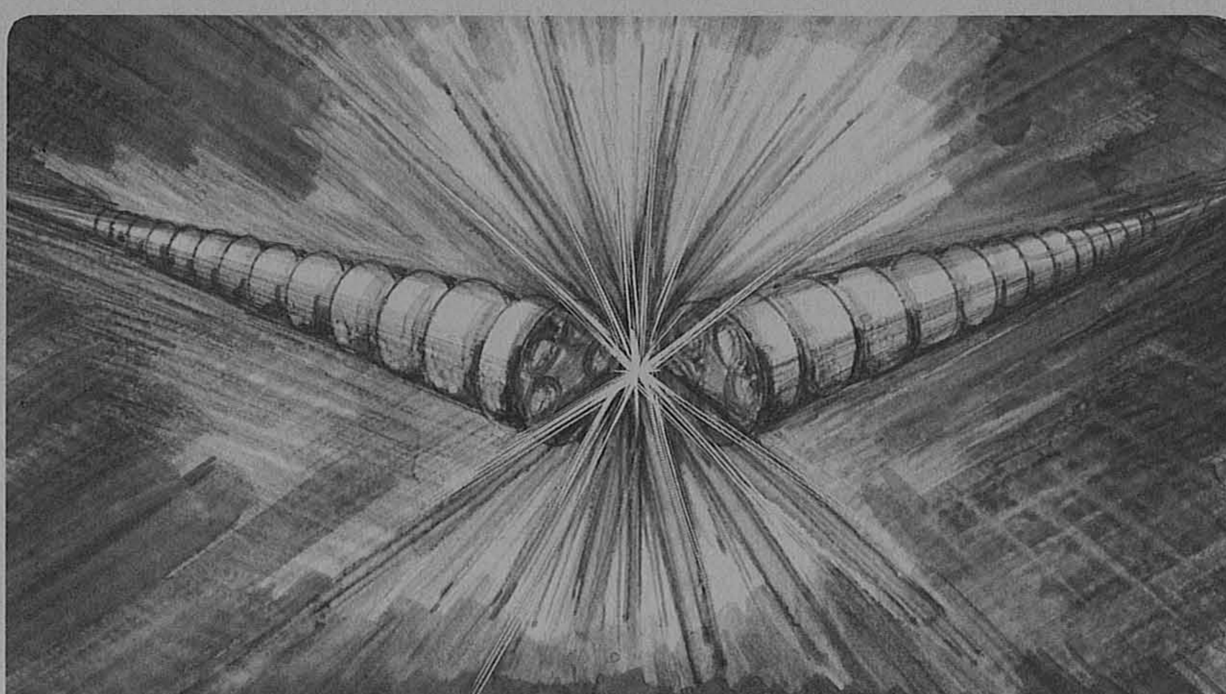

Prepared for the U.S. Department of Energy under Contract Number DE-AC03-76SF00098.

LBL-27478
ESG Note-73

RENORMALIZATION THEORY OF BEAM-BEAM INTERACTION IN ELECTRON-POSITRON COLLIDERS*

Y. H. Chin

Exploratory Accelerator Studies Group
Accelerator and Fusion Research Division
Lawrence Berkeley Laboratory
1 Cyclotron Road
Berkeley, CA 94720

July 1989

* This work was supported by the Director, Office of Energy Research, Office of High Energy and Nuclear Physics, High Energy Physics Division, Department of Energy under Contract No. DE-AC03-76SF00098.

RENORMALIZATION THEORY OF BEAM-BEAM INTERACTION IN ELECTRON-POSITRON COLLIDERS

Y. H. Chin
Exploratory Accelerator Studies Group
Lawrence Berkeley Laboratory
1 Cyclotron Road
Berkeley, CA 94720

Summary

This note is devoted to explaining the essence of the renormalization theory of beam-beam interaction for carrying out analytical calculations of equilibrium particle distributions in electron-positron colliding beam storage rings. Some new numerical examples are presented such as for betatron tune dependence of the rms beam size. The theory shows reasonably good agreements with the results of computer simulations.

Introduction

When two beams pass through each other in a colliding beam storage ring, each particle in each beam receives a transverse kick from the electromagnetic field generated by the incoming beam. This beam-beam force perturbs the particle motion, and usually causes blowup of the transverse beam size with consequent loss of luminosity. The beam lifetime may also be reduced. The understanding of the underlying physics and quantitative explanations of those phenomena are of great importance for the design of new colliding beam storage rings and for the improvement in luminosity of existing machines.

This subject has been extensively studied in terms of Hamiltonian analysis of single particle dynamics. The Hamiltonian analysis may predict orbits of regular particle motion, and may give us some criterions (e.g. Chirikov) for estimating the onset of chaotic behavior of particle orbit. It may explain the physical mechanism of the above phenomena. However, since the method is posed in terms of the behavior of a particle trajectory, it breaks down when the particle motion becomes chaotic. Therefore, it cannot be in principle applied to a beam blowup associated with chaos. It is clear that what is needed is a more statistical theory for dynamics of, not single particle, but ensemble of many particles where the chaos may be described by statistical terms. That theory would allow us to calculated particle distributions in the presence of the beam-beam interaction, which are quantities straight linked with the beam blowup and the particle loss. There have been a few attempts to derive such a theory for electron-positron colliding beam storage rings.[1-5] They all use the Fokker-Planck equation for the evolution of the particle distribution, and restrict treatment of the beam-beam interaction to the "strong-weak" case, namely the case where only the particles in the weak beam are perturbed by the beam-beam force. They also restrict themselves to a one-dimensional model except Kheifets. In spite of those simplifications in the models, only Kheifets and the author succeeded in carrying out analytical calculations of particle distributions, and have tried to compare the analytical results with results of experiments or computer simulations.

Let us explain the crux of the present problem. The Fokker-Planck equation for the particle distribution P to be solved may be written formally as

$$(\partial_\theta + \Lambda)\, P = 0\,, \qquad (1)$$

where θ is the azimuthal position in the ring, and Λ is the Fokker-Planck operator including all the effects, i.e., the beam-beam interaction, the synchrotron radiation, and so on. If we can find the Green's function as a solution of

$$\begin{aligned}(\partial_\theta + \Lambda)\, G(x,p,t|x_o,p_o,t_o) &= \delta(x-x_o)\delta(p-p_o) \quad &&\text{at } t = t_o \\ &= 0 &&\text{at } t > t_o\,,\end{aligned} \qquad (2)$$

the solution of Eq. (1) is given by

$$P(x,p,t,t_o) = \iint dx_o dp_o G(x,p,t|x_o,p_o,t_o) P(x_o,p_o,t_o)\,, \qquad (3)$$

where $P(x_o,p_o,t_o)$ is the initial particle distribution at $t=t_o$. The Green's function G which we call the "exact" Green's function includes all the orbit distortion effects and provides the exact transition probability of particle orbit, at any proceding moment, no matter whether the particle motion is chaotic or not. However, Eq. (2) is too difficult to solve exactly to obtain such Green's function. All the theories try to evaluate G with the peturbation methods, and the differences between the theories come essentially from different choices of the perturbation methods. There is one important rule in choice of the perturbation method. Namely, the method has to guarantee that a perturbation solution of any order will be smaller than the lower-order ones so that the perturbation expansion series converges. It should be emphasized that this rule is not always satisfied in any perturbation method.

The author has proposed a new perturbation method, called "the renormalization theory," to evaluate the exact Green's function systematically to a good approximation. The goal of the theory is to find a set of eigenfunctions which almost diagonalizes the system (the particle distribution here). The system may be decomposed into a set of modes. Equations of motion for the modes are usually coupled to each other by the beam-beam force. The renormalization is a procedure to rewrite those equations of motion so that the coupling between the modes as solutions of the equations becomes minimum. The renormalization theory was originally motivated to avoid the "small denominator singularities" at the centers of resonances by including orbit distortion of resonant particles due to other resonances. However, the theory turned out to be most powerful when resonances strongly interact to each other, and the system can no longer be approximated by a collection of isolated resonances. The formulation of the theory and the interpretation of its physics are found in Ref. 4. The validity of the theory is demonstrated in Ref. 5 by comparison with the results of computer simulations. In this note, we describe the outline of the theory in a rather formal way, and present some new numerical results to confirm the validity of the theory.

Renormalization Theory

We write down again the Fokker-Planck eq. for the particle distribution P in a slightly explicit form:

$$(\partial_\theta + L)\, P = L_B P\,, \qquad (4)$$

where L is the Fokker-Planck operator for all the effects except the beam-beam effect, L_B is the operator for the beam-beam effect and is a function of the beam-beam potential U. The beam-beam parameter ξ is included in the definition of U. The explicit expressions of L and L_B are given by $L_C + L_M$, and L_B, respectively, in Ref. 4. Let us decompose P into its average part $\langle P\rangle$ over the azimuthal angle ϕ in phase space and the remaining part δP fluctuating around $\langle P\rangle$:

$$P = \langle P\rangle + \delta P\,, \qquad (5)$$

$$\langle \delta P\rangle = 0\,. \qquad (6)$$

Due to the periodic boundary condition for δP in ϕ, δP can be Fourier decomposed with respect to ϕ:

$$\delta P = \sum_{m\neq 0} P_m(I,\theta)\exp(im\phi)\,, \qquad (7)$$

where I is the nominal action variable, and the m = 0 component vanishes by the definition (6). Similarly, the beam-beam potential U can be Fourier decomposed in ϕ:

$$U = \sum_{\ell=-\infty}^{\infty} U_\ell(I) \exp(i\ell\phi) . \qquad (8)$$

Equations of <P> and P_m are obtained by averaging Eq. (4) over ϕ and Fourier decomposing the remaining terms:

$$(\partial_o + L_o)\langle P\rangle = \sum_{k\neq o} M_{k,-k} U_k P_{-k} , \qquad (9)$$

$$(\partial_o + L_k) P_k = M_{ko} U_k \langle P\rangle + S_k , \qquad (10)$$

where

$$S_k = \sum_{\ell\neq o} M_{\ell,k-\ell} U_\ell P_{k-\ell} \qquad (11)$$

expresses coupling between the modes P_k. Here, $M_{k_1k_2}$, L_o, and L_k are the operators whose definitions are found in Eq. (3.6), (3.10) and (3.13) in Ref. 4, respectively. Equation (10) can be further Fourier decomposed in θ, with the result,

$$g_{k\nu}^{0^{-1}} P_{k\nu} = M_{ko} U_k \langle P\rangle + S_{k\nu} , \qquad (12)$$

where the unperturbed Green's function $g_{k\nu}^{0^{-1}}$ satisfies

$$(-i\nu - L_{ko})\, g_{k\nu}^{o} = \delta(I - I_o) . \qquad (13)$$

The explicit forms of L_{ko} and $S_{k\nu}$ are found in Eq. (4.4a) and Eq. (4.10) in Ref. 4, respectively.

The mode-coupling terms $S_{k\nu}$ become important in two cases:

1) Very weak synchrotron radiation.

In this case, the solution of Eq. (13) is approximately given by

$$g_{k\nu}^{o} = \frac{i}{\nu - k(\nu_\beta + \Delta\nu(I))} , \qquad (14)$$

where ν_β is the unperturbed betatron tune and $\Delta\nu(I)$ is the nonlinear detuning term. If we ignore the mode-coupling term $S_{k\nu}$, the solution of Eq. (12) is

$$P_{k\nu} = g_{k\nu}^{o} M_{ko} U_k \langle P\rangle = \frac{i M_{ko} U_k \langle P\rangle}{\nu - k(\nu_\beta + \Delta\nu(I))} , \qquad (15)$$

which diverges at the center of the resonance $\nu - k(\nu_\beta + \Delta\nu(I)) = 0$. If one calculates the second-order perturbation correction to $P_{k\nu}$ from $S_{k\nu}$, one finds that some terms in $S_{k\nu}$ also diverge at the same amplitude. This resonance singularity is, in fact, the result of the artificial mathematical manipulation. The singularity emerges since we have assumed that resonant particles receive only a part of beam-beam kick which creates the resonance. In reality, particles receive the total kick of beam-beam force which generate all the resonances. By the random kicks from other resonances, the particle tunes are fructuating and not strictly locked at the resonance tune. Therefore, the resonance singularity may be avoided in the real system even in the absence of the quantum fluctuation.

2) Strong coupling between resonances.

In this case, the particle motion between the resonances may be chaotic. Apparently, the exact Green's function will be very different from $g_{k\nu}^{o}$ which expresses regular orbits of resonant particles. It cannot be constructed in terms of $g_{k\nu}^{o}$ by calculating higher-order correction terms from $S_{k\nu}$, since the chaotic motion cannot be described by combination of regular motion. If one tries, then the expansion series will not converge.

Let us try the following way. We introduce the renormalized Green's function by

$$g_{k\nu} = \left[g_{k\nu}^{o^{-1}} + \Sigma_{k\nu}\right]^{-1} , \qquad (16)$$

where $\Sigma_{k\nu}$ is the operator to be determined. Substitution of Eq. (16) into Eq. (12) yields

$$g_{k\nu}^{-1} P_{k\nu} = M_{ko} U_k \langle P\rangle + S_{k\nu} + \Sigma_{k\nu} P_{k\nu} . \qquad (17)$$

Decompose $S_{k\nu}$ into the terms $S_{k\nu}^{d}$ proportional to $P_{k\nu}$ and the rest $S_{k\nu}^{nd}$:

$$S_{k\nu} = S_{k\nu}^{d} + S_{k\nu}^{nd} \qquad (18)$$

and identify

$$S_{k\nu}^{d} = -\Sigma_{k\nu} P_{k\nu} . \qquad (19)$$

Then Eq. (17) becomes

$$g_{k\nu}^{-1} P_{k\nu} = M_{ko} U_k \langle P\rangle + S_{k\nu}^{nd} . \qquad (20)$$

By the definition, the strength of $S_{k\nu}^{nd}$ does not depend on $P_{k\nu}$, namely, $S_{k\nu}^{nd}$ acts as an incoherent noise source for $P_{k\nu}$. Resonances can still cause changes in other resonances through $S_{k\nu}^{nd}$, but they are not coupled by $S_{k\nu}^{nd}$.

We have to show how to extract $S_{k\nu}^{nd}$ from $S_{k\nu}$. The physical identification is as follows. A resonance $P_{k_1\nu_1}$ can cause a change in another resonance $P_{k_2\nu_2}$ through the mode-coupling $S_{k_2\nu_2}$. The change in $P_{k_2\nu_2}$ can act back to the resonance $P_{k_1\nu_1}$ through $S_{k_1\nu_1}$, and $P_{k_1\nu_1}$ will be changed. This self-action effect should be identified as $S_{k\nu}^{d}$, since its strength depends on $P_{k_1\nu_1}$ proportionally. Mathematically, this procedure is carried out as follows. Insert the solution (17) for $P_{k\nu}$ into the definition of $S_{k\nu}$(11) and replace $S_{k-\ell,\nu}$ by Eq. (11) itself. The terms proportional to $P_{k\nu}$ is $S_{k\nu}^{d}$. In the above direct interaction approximation in which only the direct interaction between resonances (with no intermediate resonance) is taken into account, the explicit form of $\Sigma_{k\nu}$ is

$$\Sigma_{kv} = -\sum_{\ell \neq 0} \sum_{n} M_{\ell,k-\ell} U_{\ell} g_{k-\ell,v-n} M_{-\ell,k} U_{-\ell} . \qquad (21)$$

One can see from Eq. (21) that the renormalization correction term Σ_{kv} is second-order in ξ.

The physical interpretation of Σ_{kv} might be as follows. The test particle subject to the Green's function g_{kv} in the (k,v) resonance is scattered by the field $U_{-\ell}$ and is effected by the resonance $g_{k-\ell,v-n}$. Then, it is again scattered by the field U_{ℓ} to emerge at the initial resonance g_{kv}. Since the particle comes back to the initial resonance, the above trajectory going through other resonance should be included in the transition probability of the particle orbit subject to the (k,v) resonance, namely the Green's function g_{kv}.

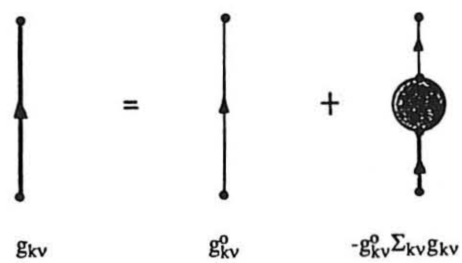

Fig. 1a Feynman diagram of Dyson's equation for the renormalized Green's function

$$g_{kv} = \left[g^{o\,-1}_{kv} + \Sigma_{kv}\right]^{-1}$$
$$= g^o_{kv} - g^o_{kv}\, \Sigma_{kv}\, g_{kv} \quad .$$

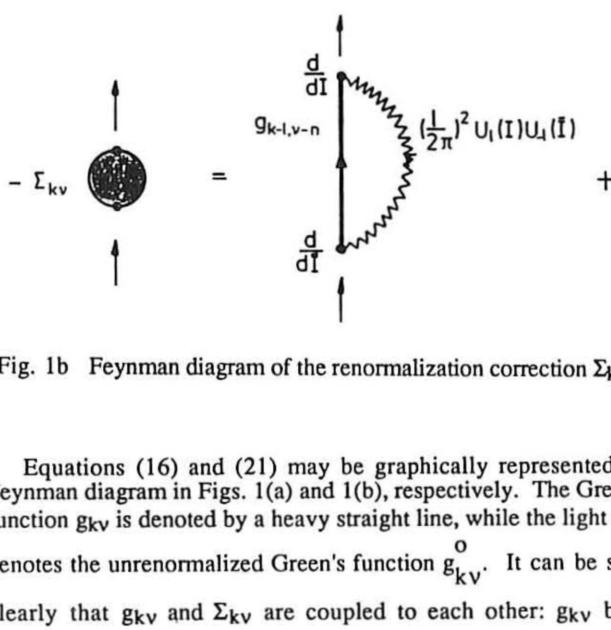

Fig. 1b Feynman diagram of the renormalization correction Σ_{kv}.

Equations (16) and (21) may be graphically represented by Feynman diagram in Figs. 1(a) and 1(b), respectively. The Green's function g_{kv} is denoted by a heavy straight line, while the light line denotes the unrenormalized Green's function g^{o}_{kv}. It can be seen clearly that g_{kv} and Σ_{kv} are coupled to each other: g_{kv} both determines and is determined by Σ_{kv}.

The solution P_{kv} may be written as consisting of two parts:

$$P_{kv}(I) = P^{coh}_{kv}(I) + P^{inc}_{kv}(I) \qquad (22)$$

with
$$P^{coh}_{kv} = g_{kv}\, M_{ko}\, U_k \langle P \rangle \qquad (23)$$

and
$$P^{inc}_{kv} = g_{kv}\, S^{nd}_{kv} \quad . \qquad (24)$$

Here P^{coh}_{kv} and P^{inc}_{kv} are the response of the resonance P_{kv} to the coherent field U_k, and the incoherent noise S^{nd}_{kv}, respectively. By being renormalized, the Green's function g_{kv} has no small denominator singularity at the center of the resonance (kv) even if the synchrotron radiation is extremely weak. It includes the most important effect from the mode-coupling, namely the coherent effect in which g_{kv} affects itself through other resonances. We can now directly compare the magnitude of perturbation terms order by order. The incoherent part P^{inc}_{kv} is formally one-order smaller in ξ than the coherent part P^{coh}_{kv}. We neglect P^{inc}_{kv} in the following procedure, and call this calculation the coherent approximation. Each mode P_{kv} couples only with <P> now, no longer with other modes P_{k_1,v_1} . Therefore the equations for <P> and P_{kv} are closed: once we know <P>, we can calculatie P_{kv}, and vice versa.

If we substitute Eq. (23) into Eq. (9) for <P>, after some approximations, we obtain

$$\left(\partial_\theta + L_o\right)\langle P \rangle = \frac{\partial}{\partial I}\mathfrak{D}(I)\frac{\partial}{\partial I}\langle P \rangle \, , \qquad (25)$$

where the explicit form of $\mathfrak{D}(I)$ is

$$\mathfrak{D}(I) = \sum_{k \neq o} \sum_{n} \left(\frac{k}{2\pi}\right)^2 U_{-k}(I) \int_o^\infty \mathrm{Re}\left(g_{kn}(I,\bar{I})\right) U_k(\bar{I})\, d\bar{I} \, . \qquad (26)$$

The term $\mathfrak{D}(I)$ may be interpretated as an additional diffusion term in amplitude space.

Approximate Solution

Equations (16) and (21) are too difficult to solve without approximations. In what follows, we truncate the perturbation expansion at $O(\xi^2)$ and $O(\gamma)$, and disregard terms proportional to any product of ξ and γ. Here $\gamma = \frac{2\gamma_y}{\omega_o}$ where γ_y is the linear radiation damping rate and ω_o is the angular revolution frequency. When resonances are well-separated, and the radiation damping is modestly strong as in LEP, the renormalization correction Σ_{kv} is overwhelmed by the radiation effects. In this region, the unrenormalized Green's functions for isolated resonances may be good approximations. Its real part is given by

$$\mathrm{Re}(g_{kv}) = \frac{|\gamma k/2|}{\left(v - k\left(v_\beta + \Delta v(I)\right)\right) + (\gamma k/2)^2} \quad . \qquad (27)$$

When resonances get closer and interact strongly with each other, the particle motion between them will be chaotic. In this strong chaotic region, Eqs. (16) and (21) can be solved between two resonances (k,v) and (k-ℓ, v-n) if we approximate the shape of $g_{kv}(I)$ by a square shape:

$$\mathrm{Re}(g_{kv}(I)) = \begin{cases} \frac{\pi}{2}\tau_{kv} & \text{if } \left|v - k\left(v_\beta + \Delta v(I)\right)\right| \le \frac{1}{\tau_{kv}} \\ 0 & \text{otherwise} \quad , \end{cases} \qquad (28)$$

where

$$\tau_{kv} = \left(\left|\frac{U_\ell(I_{kv})}{2\pi}\cdot \ell\,\Delta\nu'(I_{kv})\right|\right)^{-1/2} \frac{|k-\ell|^{1/4}}{|k|^{3/4}} \tag{29}$$

with $\Delta\nu' = \frac{d\Delta\nu(I)}{dI}$ and I_{kv} is the resonant amplitude of resonance (k,ν). The exact Green's function should be smoother, but the above function has approximately same height, width, and exactly same area π. The quantity $1/(|k|\tau_{kv})$ expresses the maximum difference between a particle tune and the resonance tune for which the particle can still be diffused by the resonance. The Green's function (28) gives an uniform transition probability in the chaotic region for chaotic particles in the present rough approximation. The chaotic (diffusive) region is confined between $\pm\, 1/(|k|\tau_{kv})$ in tune space. The diffusion rate at this region is obtained by inserting Eq. (28) into Eq. (26). The above approximation may be justified when the width of $\mathrm{Re}(g_{kv}(I))$ is larger than about 2/3 of the space $\Delta\nu_s$ of the two resonances:

$$\frac{2}{|k|\tau_{kv}} \ge \frac{2}{3}\Delta\nu_s\,, \tag{30}$$

which yields

$$\left(\left|\frac{U_\ell(I_{kv})}{2\pi}\Delta\nu'(I_{kv})\right|\right)^{1/2} \ge \frac{|kn-\ell\nu|}{3|k(k-\ell)|^{3/4}\,|\ell|^{1/2}}\,. \tag{31}$$

Before this condition is satisfied, stochastic layers or weak chaotic regions might appear between the resonances. In order to handle such intermediate regions, we need a more suble approximation. In the present treatment, we approximate a smooth transition from the Green's function (27) for the regular resonance to the Green's function (28) for the chaotic region by a sudden jump. The sudden jump is supposed to happen when the condition (31) is satisfied.

We have obtained all the Green's function for the renormalized modes. The additional diffusion rate $\mathfrak{D}(I)$ of Eq. (26) can be now calculated. In the stationary state, the solution for <P> is given by

$$\langle P(I)\rangle = K\cdot \exp\left[-\int_0^I \frac{1}{1+\mathfrak{D}(I)/(\gamma\sigma^2 I)}\,\frac{dI}{\sigma^2}\right], \tag{32}$$

where K is the normalization constant, and σ is the nominal beam size. Using this result, we can also calculate stationary P_{kv} from Eq. (23). Then, we obtain the total particle distribution.

Numercial examples are given in the next section. Here we limit the discussion only to characteristic properties of the solution (32). By taking derivative of <P> with respect to I,

$$\frac{d\langle P\rangle}{dI} = -\frac{1}{1+\mathfrak{D}(I)/(\gamma\sigma^2 I)}\,\frac{\langle P\rangle}{\sigma^2}\,. \tag{33}$$

One can see that <P> is flattened around the regions where $\mathfrak{D}(I)/(\gamma\sigma^2 I) >> 1$. If the additional diffusion regions are wide and their diffusion rates are large, one will see a significant change of <P> from the unperturbed distribution over a large range of amplitude.

Finally, to complete the calculation, we give the explicit form of the beam-beam potential produced by the Gaussian distribution:

$$U_\ell(I) = \left\{ \begin{array}{ll} 2\pi\xi(-1)^{\ell/2+1}\, 2\sigma^2 \int_0^{\frac{I}{2\sigma^2}} \frac{e^{-y}}{y} I_{\frac{\ell}{2}}(y)\,dy & \text{for } \ell = \text{even} \\ 0 & \text{for } \ell = \text{odd} \end{array} \right\} \tag{34}$$

where $I_n(y)$ is the modified Bessel function. The odd resonances are suppressed by the symmetry of the potential $U(q) = U(-q)$. The nonlinear detuning term and its derivative are

$$\Delta\nu(I) = \frac{\xi}{y}\left[1 - e^{-y} I_0(y)\right]\,, \tag{35}$$

$$\Delta\nu'(I) = -\frac{\xi}{2\sigma^2}\cdot\frac{1}{y}\left[\frac{1}{y}\left(1 - e^{-y} I_0(y)\right) - e^{-y}\left(I_0(y) - I_1(y)\right)\right]\,, \tag{36}$$

respectively, where $y = \frac{I}{2\sigma^2}$.

Comparison with Computer Simulations

In this section, we show some numerical examples of analytical particle distributions and compare them with the results of computer simulations. The computer program REBECCA (REnormalized theory of Beam-beam interaction in a Electron-positron Colliding Circular Accelerator) has been developed for computing <P> according to the theory. We compute only the averaged distribution <P>, although the total distribution can be calculated, since <P>, which is a function only of the amplitude I or r in polar coordinate, is a good measure for comparison. Besides, only <P> is needed to calculate the rms beam size (the contributions from δP are washed out when integrated over ϕ). The tracking program TRACK to simulate the beam-beam interaction has been also written for comparison. Particle distributions are averaged over ϕ to yield <P> after the tracking is finished. In all examples, γ is set to be 0.001, which is relevant to LEP at 50 GeV.

Figure 2(a) shows one quarter of the phase space trajectories calculated by TRACK for $\nu_\beta = 0.22$ and $\xi = 0.04$, where the synchrotron radiation effects are turned off specially for the plot to see regular motion of particles. This plot is taken just in the middle of the beam-beam kick so that the phase space trajectories become mirror-symmetric with respect to each coordinate. The fourth-order resonance can be seen at amplitude of about one standard deviation. This is a nonchaotic example where no chaos ensues in phase space. In fact, the calculation by REBECCA shows that the criterion (31) is satisfied between no pair of resonances, and therefore the unrenormalized Green's function (27) is used for all resonances.

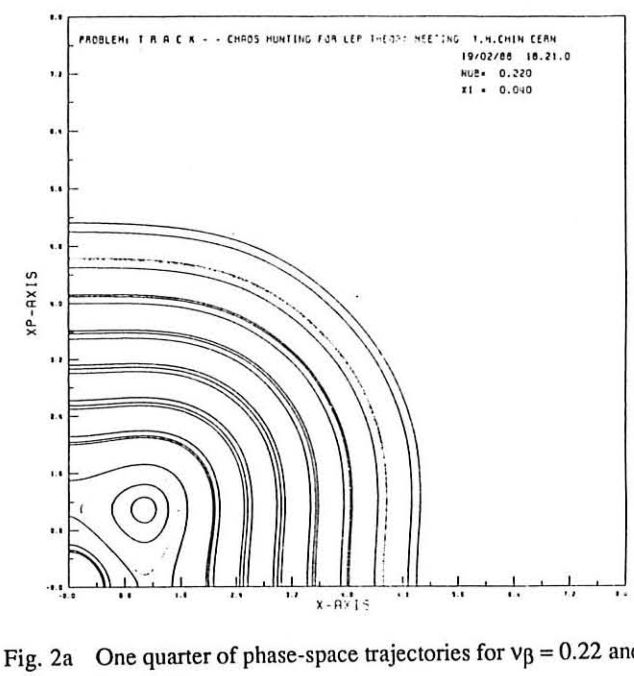

Fig. 2a One quarter of phase-space trajectories for $\nu_\beta = 0.22$ and $\xi = 0.04$.

Figure 2(b) shows the averaged particle distribution as a function of amplitude in polar coordinate in unit of one standard deviation. The solid line denotes the analytical result computed by REBECCA, while the open triangle represents the results of computer simulations. The broken line indicates the Gaussian distribution when only the linear part of beam-beam force is exerted on the beam. It is plotted as a measure to see the deviation of <P> from a Gaussian shape. A good agreement can be seen between the analytical and the computer simulation results.

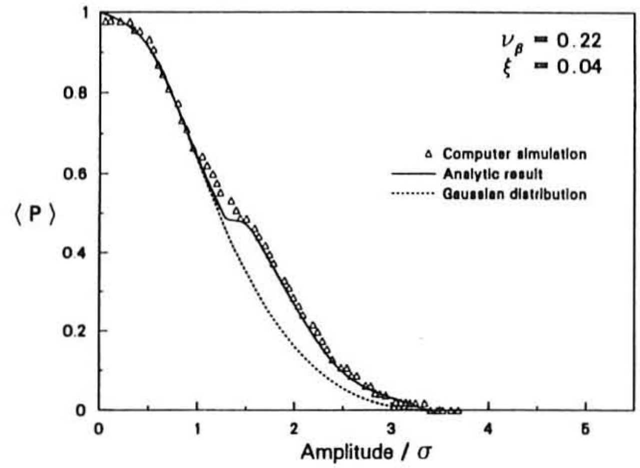

Fig. 2b Averaged particle distributions as a function of amplitude in polar coordinate.

In Fig. 3, the rms beam size is plotted as a function of the unperturbed tune ν_β for $\xi = 0.06$. In the entire tune, no chaos is obserbed in the simulations, and no chaos is predicted by REBECCA. The nomial beam size includes the effect of dynamic change in betafunction due to the linear part of beam-beam force and has a tune dependence. The analytical result is in a resonably good agreement with the simulation result except around $\nu_\beta = 0.23$ where the fourth-order resonance island is so large that the purturbation calculation for particle orbit loses its accuracy. The important point to be mentioned here is that the analytical curve has the same structure of tune dependency as the simulation curve.

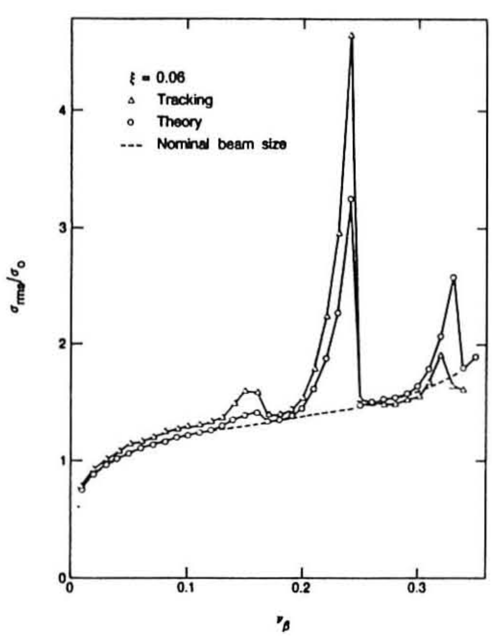

Fig. 3 The rms beam sizes as a function of ν_β for $\xi = 0.06$.

Figure 4(a) shows an example of the very chaotic phase space trajectories for $\nu_\beta = 0.15$ and $\xi = 0.17$. The synchrotron radiation is again specially turned off to see chaotic behavior of particles. The computation by REBECCA including up to the 16-th order resonances indicates the very chaotic region between 1.2 σ and 4σ at amplitude. The averaged particle distributions <P> are plotted in Fig. 4(b) where the same notations of lines as Fig. 2(b) are used. They show a good agreement except at amplitude around 2.5σ. This hard edge of the analytical distribution originates from the approximation of the renormalized Green's function by the rectangular shape in the chaotic region, although the exact Green's function should have a smoother shape. This problem may be removed by improving the approximation method.

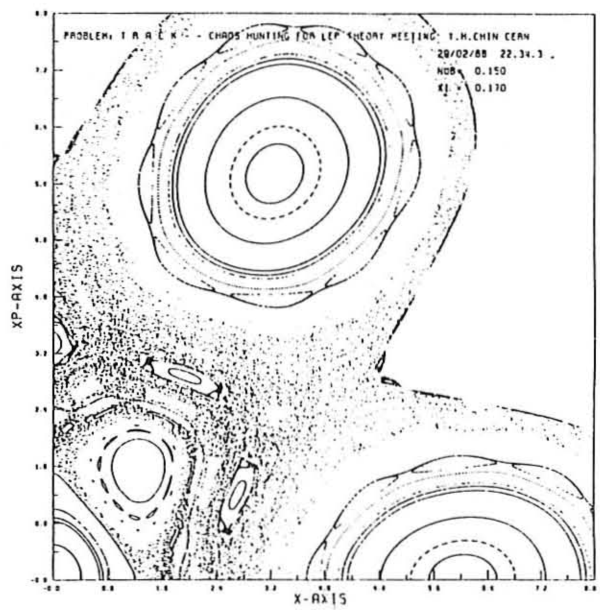

Fig. 4a One quarter of phase-space trajectories for $\nu_\beta = 0.15$ and $\xi = 0.17$.

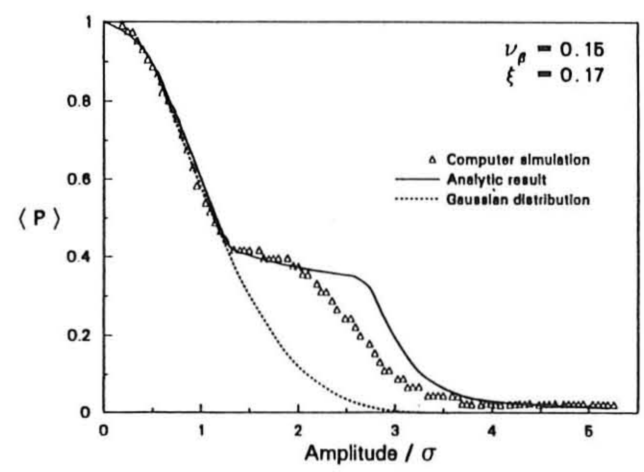

Fig. 4b Averaged particle distributions for $\nu_\beta = 0.15$ and $\xi = 0.17$.

The rms beam size is plotted as a function of the tune ν_β in Figs. 5 and 6 for $\xi = 0.16$, and $\xi = 0.18$, respectively. The chain line in Fig. 5 denotes the analytical beam size when the renormalization correction is neglected. It should be noted here that the results of the renormalized theory and those of computer simulations have the similar structure of tune dependence, although the theory sometimes overestimates or underestimates the rms beam size, while the unrenormalized theory (the closed boxes) has the different structure from the other lines. The discrepancy between the results of the renormalized theory and simulations comes mainly from the usage of the rectangular shape for the renormalized Green's function. A better approximation is desirable.

Conclusions

Let us summarize the complete algorithm to calculate an approximate stationary average distribution:

1. For all (k,ν) resonances (k=even) which satisfy

$$\nu_\beta \le \frac{\nu}{k} \le \nu_\beta + \xi \ ,$$

judge whether chaos has ensured in the vicinity, by applying the criterion (31) to all the possible pairs with (k-ℓ,ν-n) resonances (ℓ=even). If the criterion is satisfied, use the Green's function (28) for the resonance in the next procedure. If not, use the unrenormalized one (27).

2. Compute the diffusion coefficient $\mathfrak{D}(I)$ of Eq.(26).

3. Carry out the integration in Eq. (31).

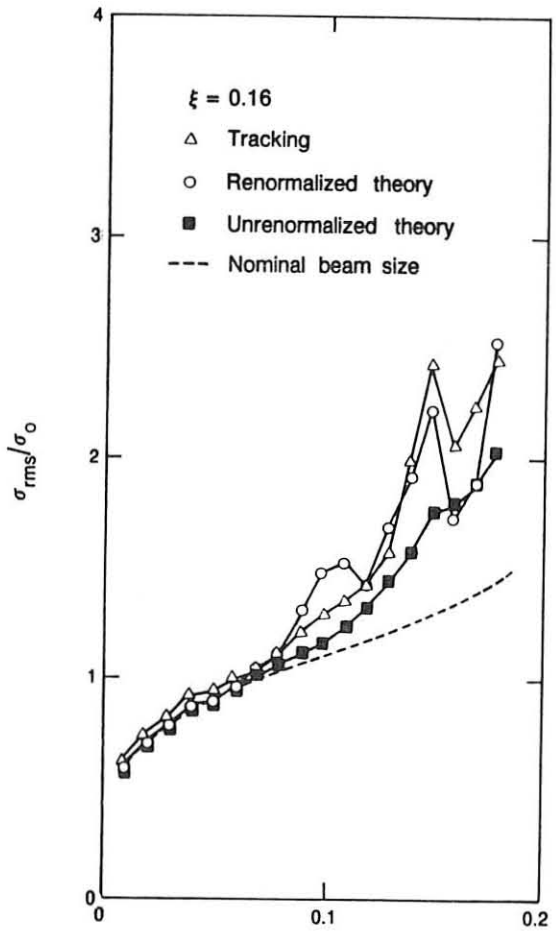

Fig. 5 The rms beam sizes as a function of ν_β for $\xi = 0.16$.

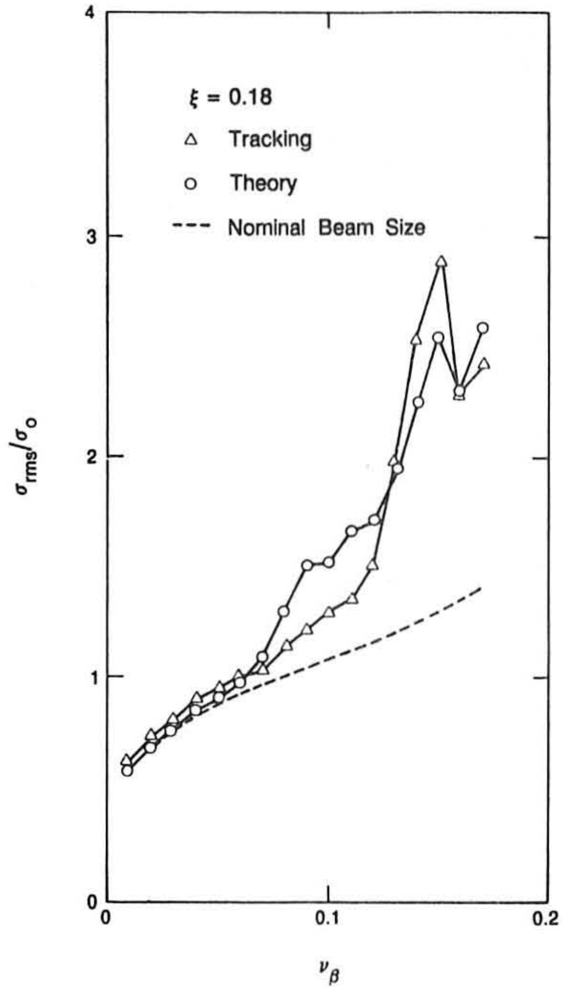

Fig. 6 The rms beam sizes as a function of ν_β for $\xi = 0.18$.

Despite of some rough approximations for the renormalized Green's function, the theory exhibits reasonably good agreements with results of computer simulations. This may imply that the present renormalization theory is a relevant perturbation method to approximate the exact Green's function in a torelable accuracy. To try to explain a beam blowup by looking at the distortion of particle orbit lies on the same line as the Hamiltonian analysis. However, by describing the orbit distortion in terms of the Green's function, we gain more capacity in the theory where statistics comes in. At the same time, the physical mechanism of a beam blowup, due to either chaos or regular resonances, is explicit in the theory. However, the present one-dimensional strong-weak beam picture is still unpractical for apllication to real machines. Further research should be made to extend the method to the two-dimensional strong-strong case.

Acknowledgment

This work was supported by the Director, Office of Energy Research, Office of High Energy and Nuclear Physics, High Energy Physics Division, Department of Energy under Contract No. DE-AC03-76SF00098.

References

1. S. Kheifets, Part. Accelerators 15, 153 (1984).

2. F. Ruggiero, Ann. Phys. (N.Y.) 153, 122 (1984).

3. J.F. Schonfeld, Ann. Phys. (N.Y.) 160, 149 (1985).

4. Y.H. Chin, KEK Preprint 87-143, 1988.

5. Y.H. Chin, LBL-25370, 1988.